Boron Distribution Analysis by Alpha-Autoradiography

Masamitsu Abe, Kazuyoshi Amano, Katsutoshi Kitamura, Jun Tateishi, and Hiroshi Hatanaka

Department of Neurosurgery and Neuropathology, Kyushu University, Fukuoka; and Department of Neurosurgery, Teikyo University, Tokyo, Japan

The distribution of the boron-10 compound, $Na_2{}^{10}B_{12}H_{11}SH$, which is now in clinical use for boron neutron capture therapy for brain tumors, was studied topographically and quantitatively in rats using neutron-induced alpha-autoradiography. Transplanted intracerebral tumors in Sprague-Dawley rats were used. In the normal brain, only a minute amount of ^{10}B (<1 μg $^{10}B/cm^3$) was found in the brain parenchyma, except for the infundibulum and area postrema. Boron-10 accumulated in the brain tumors. The tumor-to-blood concentration ratio of ^{10}B increased with time after injection and reached unity 12 hr after injection. The tumor concentration calculated at that time was 18 μg $^{10}B/cm^3$. This study clearly shows that this ^{10}B compound accumulates in the transplanted rat tumors in the brain and that tumor concentration and tumor-to-blood ratio of ^{10}B can provide a sufficient condition for brain tumor treatment.

J Nucl Med 27:677–684, 1986

An ideal therapy for brain tumors would be one whereby all tumor tissue was selectively destroyed without causing damage to the functioning brain. Boron neutron capture therapy for brain tumors is a radiation therapy modality employing the administration of a boron-10 (^{10}B) compound, which accumulates in the tumor tissue, followed by irradiation with low-energy neutrons (*1,2*). Boron-10 in or adjacent to the tumor cells disintegrates after capturing a neutron and the high-energy heavy particles produced destroy only the tumor cells in close proximity to it. For the boron neutron capture treatment to be "ideal," it must meet the requirement that ^{10}B be distributed evenly within the tumor and none outside it. After many kinds of ^{10}B compounds were made and tested (*3–5*), $Na_2{}^{10}B_{12}H_{11}SH$ was selected and has been used for human brain tumor treatment (*6–8*).

The distribution of this compound was studied by Hatanaka (*8*), using tritium-labeled autoradiography, and by Matsuoka et al. (*9*) and by Amano et al. (*10*), using neutron-induced alpha-autoradiography. They made no quantitative analysis, however, of ^{10}B distribution. We studied time-sequential ^{10}B distribution in the transplanted brain tumors quantitatively. Furthermore, to estimate any undesirable effect on tissues surrounding the brain, we also investigated ^{10}B distribution in specimens of several tissues outside the brain.

Received May 16, 1985; revision accepted Dec. 31, 1985.

For reprints contact: Masamitsu Abe, MD, Stereotactic Neurosurgery, Massachusetts General Hospital, 15 Parkman ACC-324, Boston, MA 02114-2280.

MATERIALS AND METHODS

Intracerebral tumors were produced by implantation of the glioma cell RGC6, a clone derived from a rat glioma induced with *N*-nitrosomethylurea (*11*). Prior to implantation this clone was trypsinized, washed in phosphate buffer, and suspended in 0.5% agar solution at 37°C. Cell concentration was adjusted to 10^5 cells/μl suspension medium. Forty Sprague-Dawley (SD) rats, weighing 150–200 g at 12–16 wk, were anesthetized with an i.p. administration of sodium pentobarbital (3 mg/100 g body weight) and fixed in a frame. Under sterile conditions, a small burr hole was made with a dental drill on the right coronal suture 4 mm lateral from the midline. A microsyringe was inserted into the brain and 5 μl of cell suspension was injected at the depth of 5 mm below the skull. During these procedures, the cell suspension and microsyringe temperature was maintained at 37°C. The skin incision was sutured and the animals were allowed to recover after the injection.

Administration of ^{10}B and Neutron-Induced Alpha-Autoradiography

Normal controls, weighing 200–300 g at 24–48 wk, and tumor-bearing animals, 3–4 wk after the implan-

tation, were anesthetized with an i.p. administration of sodium pentobarbital (3 mg/100 g of body weight). Sodium mercaptoundecahydrododecaborate, $Na_2{}^{10}B_{12}H_{11}SH$ (^{10}B enriched to 96% and containing 5% of H_2O, Shionogi Research Laboratory), of 50 or 100 μg ^{10}B/g body weight dissolved in distilled water to become isotonic (0.1 *M* solution), was injected into the tail vein of each of the controls and tumor-bearing rats. The injection was performed very slowly over 5–10 min. These animals were killed sequentially at 1–48 hr after injection by exsanguination under ether anesthesia. The brains were quickly removed and cut into four coronal sections. The sections showing the largest cut surface area of the tumors were frozen in freon and cooled in a liquid nitrogen bath. Several sections were cut in 8 μm thicknesses using a cryocut cryostat microtome, mounted directly onto the films and glass slides, and promptly placed in a desiccator to dry for 1.5 hr over fresh P_2O_5 (*12,13*). Cellulose nitrate films (LR115 type and CN85) were used for alpha-autoradiography. The rest of the brain sections were fixed in 10% formalin and processed for histologic examination. In two normal rats, serial coronal sections were cut from the frontal pole to the medulla oblongata. At each 250-μm interval, two sections were taken as samples—one section mounted on a glass slide, and the other on the film. Blood evacuated from the heart was diluted with ten volumes of liquid gelatin and allowed to solidify. Sections were then cut and mounted on the films by the same procedure. Liver, pituitary glands, trigeminal ganglia, eyes, skin, and temporal muscle were also processed in the same way as the brain.

Three sets of mounted sections and films were taken to Musashi Institute of Technology Medical Reactor and exposed to thermal neutron beams. Neutron flux delivered was 1.2–2.1 $\times$ 10^{12} n/cm^2 to the first set, 5.7–11 $\times$ 10^{12} n/cm^2 to the second set, and 8.8–35 $\times$ 10^{12} n/cm^2 to the final set. The actual neutron flux to each tissue section was later calculated by measuring the radioactivities of gold foils placed near the section during the irradiation. The sections on the films were then stained with hematoxylin-eosin (HE) and examined both macroscopically and under a microscope. The films were etched by soaking in 60°C 2.5N NaOH for 20 min. Pits were formed in the films at the sites of tracks of alpha or lithium particles from ^{10}B disintegration, and could be readily seen under a microscope. The pits were seen to the naked eye as cloudiness in the film. The tissue sections were damaged by the strong alkalinity during etching. The stained tissue section disappeared when the pits emerged. The distribution of pits was correlated to the histologic picture using the superimposition technique (*10*). Microphotographs were taken before and after etching while the film was fixed to the microscopic table. Sections on the glass slides were stained with Nissl or Klüver-Barrera (KB).

Quantitative Analysis of ^{10}B

The number of nuclear reactions occurring in 1 cubic centimeter during thermal neutron irradiation is given by (*8,14*):

$$R = \Phi \Sigma \iota \sigma a i \frac{Pi}{Ai} N$$

Φ = Neutron flux, cm^{-2};
σa = Absorption cross section, cm^2;
P = Concentration of nuclide, g cm^{-3};
A = Atomic weight, g;
N = Avogadro number 6.03 $\times$ 10^{23}.

At a given neutron flux, the number of $^{10}B(n, \alpha)$ reactions is the number of tracks in tissue containing ^{10}B, less the number of tracks in the same tissue without ^{10}B, and is in proportion to the concentration of ^{10}B.

To make a standard curve, a standard solution of 521 μg ^{10}B/ml was made with 10.0 mg of ^{10}B compound ($Na_2{}^{10}B_{12}H_{11}SH$, ^{10}B enriched in 96%, containing 5% H_2O) dissolved in 10 ml of distilled water. The solution was then diluted with liquid gelatin to the concentrations of 5.21, 26.0 and 52.1 μg ^{10}B/cm^3. These concentrations were frozen and 8-μm-thick sections of each were cut and mounted on the film and exposed to thermal neutrons of 1.2 $\times$ 10^{12} n/cm^2. The number of tracks on the film with a section containing no ^{10}B was counted and subtracted from the number of tracks on the film with sections containing ^{10}B. This number was then plotted as a function of ^{10}B concentration. The best straight line was fitted to these points (Fig. 1). The equation of this line was:

$$x = 1.38n - 0.87,$$

x = ^{10}B concentration μg ^{10}B/cm^3
n = Number of tracks/10^3 μm^2,

which was used to calculate the ^{10}B concentration.

Counting of tracks in the microphotographs was performed at a magnification of 100 to 200 $\times$ over an area of 1–5 $\times$ 10^4 μm^2. The mean and s.d. of ^{10}B concentration were calculated for from three to ten areas per section due to the varying ^{10}B density of the tumor sections.

Boron-10 concentration in the liver and the blood was analyzed chemically at the Shionogi Research Laboratory and compared with the corresponding autoradiographic analysis.

RESULTS

Tumors grew in 32 of the 40 rats that had transplants of tumor cells. Most of the tumors developed in the right caudate nucleus and had a global shape. Histologic examination showed a relatively sharp demarcation of the tumors and, in most, central coagulation necrosis.

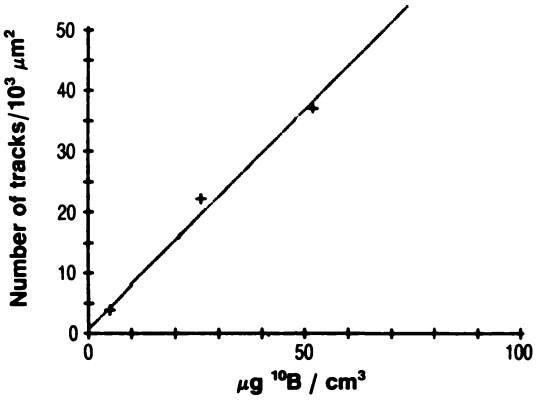

FIGURE 1
Most appropriate construction of standard curve showing linearity between standards of ^{10}B concentration and average numbers of tracks at thermal neutron flux of 1.2×10^{12} n/cm²

An even distribution of mildly or moderately dilated capillaries was observed except in the necrotic part.

Boron-10 Distribution Analysis by Alpha-Autoradiography

Animals without ^{10}B injection. A small number of tracks was found on the film which contained no tissue section at all. Most of these tracks resulted from reactions between N_2 in the air and thermal neutrons ($^{14}N(n, p)^{14}C$ reaction). When the tissue sections were sandwiched between two layers of film, the number of these background tracks became negligible. Film under tissue section of uninjected animals showed a small number of tracks when a large amount of neutron flux was given. These tracks resulted from reactions between thermal neutron and atoms such as N, Na, Cl, etc., in the tissue.

Animals with ^{10}B injection. Normal rat brain. Whitish clouded areas resulting from the accumulation of etched tracks correspond to the choroid plexuses and blood vessels (Fig. 2). Clouded areas were not found on the film under the brain parenchyma except at the infundibulum and area postrema where mild cloudiness was found. Under a microscope, a large number of etched tracks was found in the place corresponding to the choroid plexuses and blood. A small to relatively large number of etched tracks were found in the ependyma, arachnoid, pia mater, and vessel walls in the subarachnoid space (Fig. 3). Although the number of tracks in the gray matter was greater than in the white matter, both of them were very small.

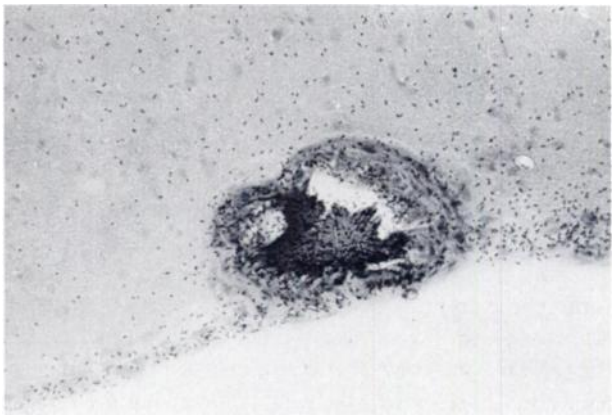

FIGURE 3
Alpha-autoradiograph of blood vessel in subarachnoid space of normal brain shown by superimposition technique. Many rod-shaped tracks accumulate on blood, vessel wall and meninges × 264

Transplanted rat brain tumors. The sections of brain tumors and their track-etch pictures, 2, 6, 24, and 48 hr after injection, are shown in Fig. 4. Cloudiness indicating concentration of ^{10}B in the tumors is observed. Inside the tumors which showed central necrosis, more ^{10}B was found in the central necrosis than in the viable tumor tissue from as soon as 2 hr, to as long as 48 hr after injection. Outside of the necrosis more ^{10}B was found in the viable tissue of the periphery of the tumor than in the central viable tumor tissue. In the case of a tumor protruding into the cerebral ventricle, less ^{10}B was found in the protruding section than in the intracerebral area. In the case of a very large tumor with marked brain edema, ^{10}B accumulated in the edematous brain as well as in the tumor. The grade and extent of ^{10}B concentration in the brain surrounding the tumor varied with the tumors. No clear relation was found between the grade and extent of ^{10}B outside the tumor and the time after injection.

In a high-power microscopic picture in which the etched tracks were superimposed on the tumor cells, the tracks were seen to be almost evenly distributed.

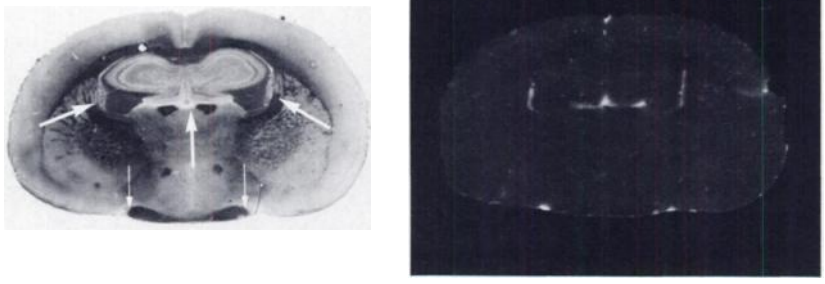

FIGURE 2
Coronal section of normal brain of rat killed 18 hr after injection of ^{10}B compound. On left is section of K.B. stain and on right is track-etch picture. Clouded areas correspond to choroid plexuses (large arrows) and blood vessels (small arrows) × 5.3

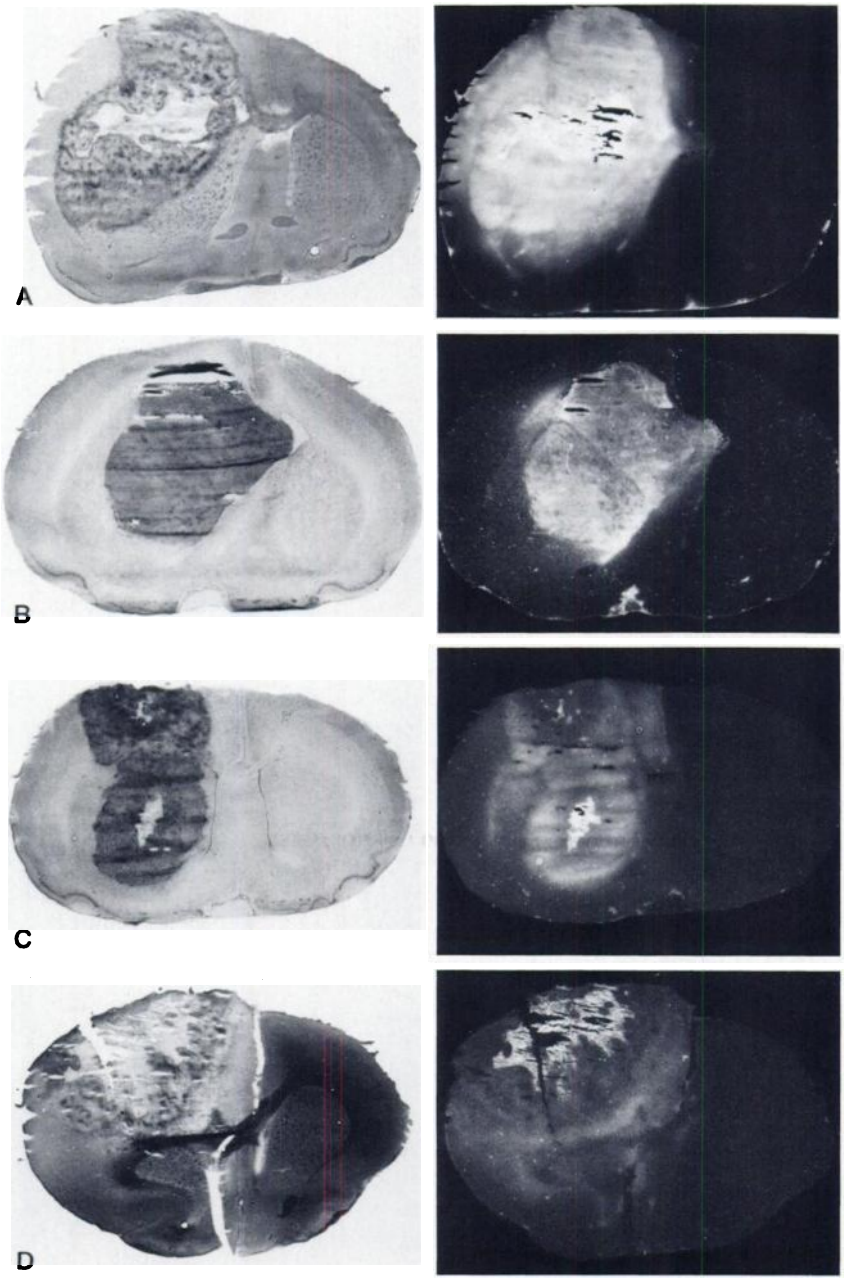

FIGURE 4
Sections of transplanted brain tumors (Nissl or K.B. stain) on left side, and track-etch pictures on right side. A: Two hours after injection. Thick cloudiness is seen in tumor and brain adjacent to tumor. Thicker cloudiness corresponds to central necrosis of tumor. K.B. × 5.3. B: Six hours after injection. Nissl × 5.3. C: Twenty-four hours after injection. Thicker cloudiness is seen in central necrosis and peripheral part of tumor. Nissl × 5.3. D: Forty-eight hours after injection. Thick cloudiness remains in central necrosis and relatively thick cloudiness is seen in peripheral tumor tissue and in edematous brain. K.B. × 5.3

No particular accumulation of ^{10}B in the cell membrane or nucleus was noted (Fig. 5). In the border zone between tumor and brain, the number of tracks decreased gradually from within the tumor outward to the brain with no definite line of demarcation.

Other tissues. Many tracks were seen in the sections of the posterior lobe as well as the anterior lobe of the pituitary gland and trigeminal ganglion. In the eyes, many tracks were found in the sections of cornea, sclera, and choroidea but few tracks on the lens, vitreous body, and retina. Many tracks were distributed evenly on the liver sections. A few tracks were seen on the muscle fiber sections. Many tracks were seen in the skin sections, especially in fibrous connective tissue.

Quantitative Analysis of ^{10}B

Blood and liver. Boron-10 concentration in the blood and the liver as analyzed by autoradiography (μg $^{10}B/cm^3$) and by the chemical method (μg $^{10}B/g$) is shown in Table 1. No large discrepancy was observed between the figures calculated by the two methods. The concentration in the liver correlated to that in the blood.

Brain and brain tumors. Boron-10 concentration in normal brain parenchyma was 1 μg $^{10}B/cm^3$ 1 hr after injection and extremely low 12 hr after injection. Concentration was slightly higher in area postrema and infundibulum (Table 2). Except for these regions, no areas of notable concentration were found in the normal brain parenchyma. Boron-10 concentration in tu-

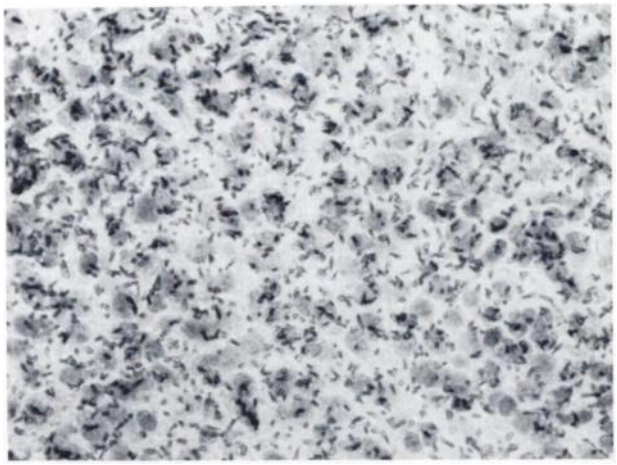

FIGURE 5
Alpha-autoradiograph of tumor cells by superimposition technique. Many rod-shaped tracks are almost evenly distributed. H.E. × 660

mor tissue is represented by mean concentration in viable tumor tissue, excluding necrosis. Regional differences of concentration within a tumor are shown as standard deviation. Concentration in the brain distant from the tumors was very low (Table 3).

TABLE 1
Boron-10 Concentration in Blood and Liver of Rats: Autoradiographical Analysis (μg ^{10}B/cm^3) and Chemical Analysis (μg ^{10}B/g)

Hours after infusion	ARG analysis		Chemical analysis	
	Blood	Liver	Blood	Liver
100 μg ^{10}B/g injected				
1	86.5	58.9		
1.5	98.3	101.5		
1.5	106.6	222.5	119.5	257.6
2	91.8	126.0	70.8	140.3
3	60.7	47.9		
3	63.2	31.2		
6	39.6	21.8		
6	22.1	10.9	15.7	19.9
6.5	39.8	22.7		
6.5	25.7	12.6		
18	6.2	6.7	8.8	6.2
19.5	9.8	2.7	5.9	4.8
24	7.1	23.0	6.3	17.2
24	12.0	7.6	8.0	6.1
48	3.5	3.3	3.8	2.9
48	3.0	1.4	3.1	4.8
50 μg ^{10}B/g injected				
12	14.2	6.5		
12	7.4	8.3		
18	8.2	10.8		
Noninjected				
	NG*	NG	1.0	1.0
	NG	NG		
	NG	NG		

*Negligible quantity.

TABLE 2
Boron-10 Concentration (μg ^{10}B/cm^3) in Normal Rat Brain

Hours after infusion	Brain	Infundibulum	Area postrema
100 μg ^{10}B/g injected			
1	1.0		
19.5	NG*		
50 μg ^{10}B/g injected			
12	NG	1.2	0.5
18	NG	0.5	0.2

*Negligible quantity.

Both ^{10}B concentration in the tumors and tumor-to-blood concentration ratios of the rats injected with 100 μg ^{10}B/g were plotted according to elapsed time, and the most appropriate curves were constructed respectively (Figs. 6 and 7). Boron-10 concentration in the tumors gradually decreased with time after injection and reached 20 μg ^{10}B/cm^3 at 10 hr after injection. The tumor-to-blood ratio of ^{10}B concentration increased with time after injection and reached unity at 12 hr after injection. The tumor concentration calculated at that time was 18 μg ^{10}B/cm^3.

Other tissues. Boron-10 concentration in tissues adjacent to the brain is tabulated in Table 4. Concentration in these tissues except for retina and muscle was relatively high, although it was lower than that in the brain tumors.

DISCUSSION

Boron-10 is a nonradioactive isotope. In order to identify ^{10}B distribution, ^{10}B compound can either be labeled with tritium (beta-autoradiography) (*15*) or the sample can be irradiated with thermal neutrons and neutron-induced alpha-autoradiography can be performed. The former technique is complicated by the possibility that the ^{10}B compound may change in struc-

TABLE 3
Boron-10 Concentration (μg ^{10}B/cm^3) in Tumors and Tumor-to-Blood Ratios of Rats Injected with 100 μg ^{10}B/g

Hours after infusion	Tumor*	Distant brain	Tumor/ blood
2	93.5 ± 22.9	1.7	0.89
3	36.4 ± 3.6	0.5	0.60
6	23.0 ± 9.9	0.3	1.04
24	13.7 ± 2.2	NG†	1.14
48	6.5 ± 1.1	NG	2.17

*Mean ± s.d. in one tumor.
†Negligible quantity.

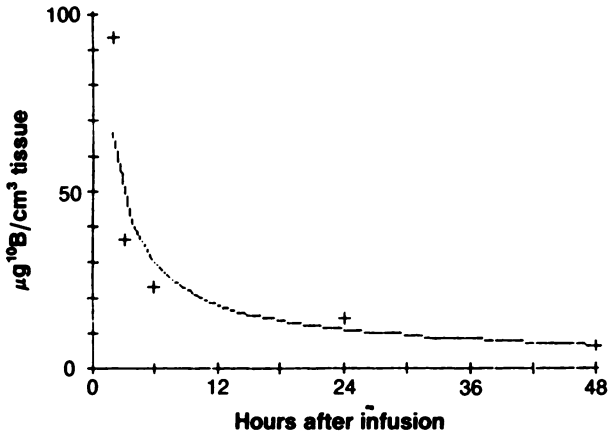

FIGURE 6
Mean ^{10}B concentration in tumors in rats after i.v. infusion of 100 μg ^{10}B/g

ture before or after labeling (*8*). The latter technique has been hampered by the background artifacts which make identification of the actual location of the ^{10}B difficult. A solid state particle detector has been developed, however, that overcomes this difficulty (*16,17*). Accumulation of ^{10}B in the transplanted subcutaneous and intracerebral tumors was shown by Matsuoka et al. (*9*) using this technique. Etching of the film is essential to make visible the path of the heavy particles. Since the tissue section is destroyed in the very process of etching (which is necessary to visualize the ^{10}B distribution), the histologic section cannot be seen at the same time as the distribution of the ^{10}B. This weakness was overcome by a superimposition technique, and a microscopic study of ^{10}B distribution was carried out by Amano et al. (*10*).

Sodium mercaptoundecahydrododecaborate ($Na_2{}^{10}B_{12}H_{11}SH$, mol wt 210) is water soluble and is strongly bound to serum albumin in the blood (*18*). This compound is, therefore, thought not to enter the brain but to enter brain tumors which are devoid of the strongly bound to serum albumin in the blood (*18*). blood-brain barrier (*19*). The results in the present

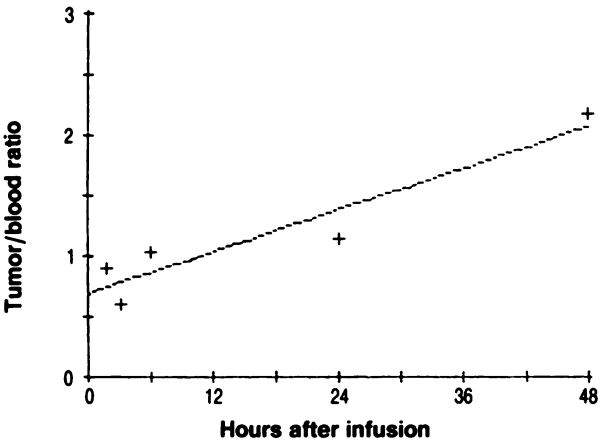

FIGURE 7
Tumor-to-blood concentration ratios of ^{10}B

TABLE 4
Boron-10 Concentration (μg ^{10}B/cm³) in Tissues Adjacent to Brain

Hours after infusion	Trigeminal nerve (ganglion)	Pituitary gland	Cornea	Retina	Muscle	Skin
100 μg ^{10}B/g injected						
1	11.3	4.0	29.8	1.5		
1.5	3.7	14.6	33.7	0.3		
1.5	31.2 (59.8)	22.4	12.3	10.5		
2	9.0	13.4	44.1	1.7		
3	5.0	3.6	1.0	NG		
3	4.6	1.3	1.5	0.8		
6	7.3	7.9	9.8	3.9		
6	2.0	1.7	1.9	1.9		
6.5	2.7	2.0	3.1	1.2		
6.5	3.5	4.5	2.3	0.3		
18	0.1	2.1	2.8	0.8		
19.5	NG*	1.7	NG	NG		
24	0.6	1.9	0.5	NG		
24	0.2	2.0	1.3	NG		
48	NG	1.7	3.6	NG		
48	0.1	NG	2.2	1.0		
50 μg ^{10}B/g injected						
12	0.6 (2.5)		4.7	0.1	NG	2.2
12		3.5	2.2	NG	0.5	3.6
18	NG	41	6.6	0.2	1.8	6.9

*Negligible quantity.

study confirmed this by showing that an almost negligible amount of ^{10}B was found in the brain parenchyma while ^{10}B accumulated in the tumors. A slightly higher concentration was seen in the area postrema and infundibulum, where blood vessels are more permeable than in the rest of the brain parenchyma (*20*). A large amount of ^{10}B was found in the choroid plexus, which is devoid of a barrier. A small amount of ^{10}B collected in the vessel wall in the subarachnoid space, arachnoid and pia mater. It was probably derived from ^{10}B in the cerebrospinal fluid (*8,21*).

Some other features of ^{10}B distribution in a tumor are demonstrated in the present study. In the tumors with central necrosis, ^{10}B concentration in the central viable tumor tissue was less than that in the peripheral tumor tissue. This may be attributable to slower blood flow in the central part (*22*). Boron-10 accumulated in the central necrosis 2 hr after administration and remained until 48 hr after administration. A similar phenomenon was found in our study using horseradish peroxidase and Evans blue. In the case with marked brain edema surrounding the tumor, the concentration in the edematous brain was relatively high. Although to the naked eye ^{10}B seemed to be localized in the tumor, under the microscope, it was not at all localized in the tumor cells; rather, ^{10}B concentration decreased gradually from within the tumor outward to the brain. It is likely that this ^{10}B compound has some affinity to the brain tumor because concentration in the tumor

was higher than in extracerebral tissues which were also devoid of the barrier. However, it seems that this ^{10}B compound does not have such a selective affinity that it is attracted only to the tumor cells. Boron-10 distribution at the cellular level is also important because the effect on the tumor cells of heavy particles resulting from ^{10}B disintegration varied according to the location of the ^{10}B in the tumor cells. Unfortunately, the present study could not clarify the exact location of ^{10}B at the cellular level.

Among the extracerebral tissues we studied, ^{10}B accumulated in the pituitary gland, trigeminal ganglion, cornea, sclera, and choroidea of the eyes and the skin. Concentration in the trigeminal nerve which enjoys a blood-nerve barrier was lower than in the trigeminal ganglion which is devoid of the barrier (*23*). Concentration in the retina which enjoys a blood-retinal barrier was as low as in the brain parenchyma. Nevertheless, ^{10}B does not necessarily accumulate in all tissues which are devoid of a barrier. Only a small amount of ^{10}B was found in the muscle, while a large amount was found in the fibrous connective tissue, which may suggest that this ^{10}B compound collects readily on fibrous protein.

Regarding clinical application of boron neutron capture therapy, ^{10}B concentration in blood is as important as its distribution and concentration in the tumor. One of the main causes of the discouraging results of the first clinical trials was the damage done to the vascular wall by the large amounts of ^{10}B in the blood during neutron irradiation (*24*). However, boron compounds that yield a higher concentration in the tumor than in the blood have been investigated thereafter (*2,4,19,25*). In the present study, the tumor-to-blood concentration ratio increased with time after injection and reached unity 12 hr after injection. This ratio and the distribution of ^{10}B are much better than those in the first clinical trials (*24*) and in experiments using other boron compounds (*5,26,27*). Unity of tumor-to-blood ratio is sufficient for treatment because even at unity, as Kitao (*28*) or Rydin et al. (*29*) reported, the radiation dose absorbed by the capillary wall is calculated to be only one-third of the tumor dose. Tumor can be destroyed without significant vascular injury of the normal brain.

The data presented in this study show that this boron compound can yield a sufficient tumor concentration and tumor-to-blood ratio for the neutron capture therapy. Uneven distribution in the tumor and relatively high concentration in the brain edema are problems to be addressed before being able to achieve highly selective destruction of tumor cells.

ACKNOWLEDGMENTS

The authors thank Dr. Tetsuji Chou for technical help with the alpha-autoradiography and Dr. Tetsuo Matsumoto for the thermal neutron irradiation.

This work was supported in part by a grant-in-aid for fundamental scientific research from the Ministry of Education.

REFERENCES

1. Sweet WH, Javid M: The possible use of neutron-capturing isotopes such as boron-10 in the treatment of neoplasms. *J Neurosurg* 9:200–209, 1952
2. Zamenhof RG, Murray BW, Brownell GL, et al: Boron neutron capture therapy for the treatment of cerebral gliomas. 1. Theoretical evaluation of the efficacy of various neutron beams. *Med Phys* 2:47–60, 1975
3. Soloway AH: Boron compounds in cancer therapy. In *Progress in Boron Chemistry*, Vol. 1, Steinberg H, McClosky AL, eds. New York, Pergamon Press, 1964, pp 203–234
4. Soloway AH, Hatanaka H, Davis MA: Penetration of brain and brain tumor. VII. Tumor-binding sulfhydryl boron compounds. *J Med Chem* 10:714–717, 1967
5. Soloway AH, Messer JR: Determination of hydrolytically-stable boron hydrides in biological materials. *Anal Chem* 36:433–434, 1964
6. Hatanaka H, Amano K, Kamano S, et al: Boron neutron capture therapy vs photon beam for malignant brain tumors—12 years' experience. In *Modern Neurosurgery*, Vol. 1, Brock M, ed. Berlin Heidelberg, Springer-Verlag, 1982, pp 122–136
7. Hatanaka H, Sano K: A revised boron-neutron capture therapy for malignant brain tumors. I. Experience on terminally ill patients after cobalt-60 radiotherapy. *Z Neurol* 204:309–332, 1973
8. Hatanaka H, Watanabe T: Treatment of brain tumors with slow neutron. *Geka-Shinryo (Surg Diag Treat)* 12:1041–1055, 1970
9. Matsuoka O, Hatanaka H, Miyamoto M: Neutron capture whole body autoradiography of ^{10}B compounds. *Acta Pharmacol Toxicol* (Suppl 1) 41:56–57, 1977
10. Amano K, Sweet WH: Alpha-autoradiography of ^{10}B compound distribution in tissue by use of superimposition technique. *Nippon Acta Radiol* 33:267–272, 1973
11. Benda P, Someda K, Messer J, et al: Morphological and immunochemical studies of rat glial tumors and clonal strains propagated in culture. *J Neurosurg* 34:310–323, 1971
12. Spriggs TLB, Lever JD, Rees PM, et al: Controlled formaldehyde-catecholamine condensation in cryostat sections to show adrenergic nerves by fluorescence. *Stain Techn* 41:323–327, 1966
13. Stumpf WE, Roth LJ: High resolution autoradiography with dry mounted, freeze-dried frozen sections. *J Histochem Cytochem* 14:274–287, 1966
14. Fairchild RG, Tonna EA, Seibold CT: Development of a low-background neutron autoradiographic technique. *Radiation Res* 30:774–787, 1967
15. Zervas NT, Soloway AH: The microscopic distribution of water soluble compounds by autoradiography. *J Neuropathol Exp Neurol* 23;151–155, 1964
16. Becker K, Johnson DR: Nonphotographic alpha autoradiography and neutron-induced autoradiography. *Science* 167:1370–1372, 1970
17. Cole A, Simmons DJ, Cummins H, et al: Application of cellulose nitrate films for alpha autoradiography of bone. *Health Phys* 19:55–56, 1970

18. Nakagawa T, Nagai T: Interaction between serum albumin and mercaptoundecahydrododecaborate ion. *Chem Pharm Bull* 24:2934–2954, 1976
19. Tolpin EI, Wellum GR, Dohan FC Jr, et al: Boron neutron capture therapy of cerebral gliomas. *Oncology* 32:223–246, 1975
20. Bradbury M: *The Concept of a Blood-Brain Barrier*, New York, John Wiley & Sons, 1979
21. Shabo AL, Maxwell DS: The subarachnoid space following the introduction of a foreign protein: An electron microscopic study with peroxidase. *J Neuropathol Exp Neurol* 30:506–524, 1971
22. Blasberg R, Patlak C, Shapiro W, et al: Metastatic brain tumors: Local blood flow and capillary permeability. *Neurology* 29:549, 1979 (abstr)
23. Jacobs JM, Macfarlane RM, Cavanagh JB: Vascular leakage in the dorsal root ganglia of the rat, studied with horseradish peroxidase. *J Neurol Sci* 29:95–107, 1976
24. Asbury AK, Ojemann RG, Nielsen SL, et al: Neuropathologic study of fourteen cases of malignant brain tumor treated by boron-10 slow neutron capture radiation. *J Neuropathol Exp Neurol* 31:278–303, 1972
25. Brownell GL, Zamenhof RG, Murray BW, et al: Boron neutron capture therapy. In *Therapy in Nuclear Medicine*, Section 18, Spencer RS, ed. New York, Grune & Stratton, 1978, pp 205–222
26. Hatanaka H, Soloway AH, Sweet WH: Incorporation of pyrimidines and boron analogues into brain tumour and brain tissue of mice. *Neurochirurgia* 10:87–95, 1967
27. Locksley HB, Sweet WH: Tissue distribution of boron compounds in relation to neutron-capture therapy of cancer. *Proc Soc Exper Biol Med* 86:56–63, 1954
28. Kitao K: A method for calculating the absorbed dose near interface from $^{10}B(n,\alpha)\ ^{7}Li$ reaction. *Radiation Res* 61:304–315, 1975
29. Rydin RA, Deutsch OL, Murray BW: The effect of geometry on capillary wall dose for boron neutron capture therapy. *Phys Med Biol* 21:134–138, 1976